Journal of Water Process Engineering 46 (2022) 102514

Contents lists available at ScienceDirect

Journal of Water Process Engineering

journal homepage: www.elsevier.com/locate/jwpe

An efficient green photo-Fenton system for the degradation of organic pollutants. Kinetics of propranolol removal from different water matrices

W. Remache [a,b,c,1], D.R. Ramos [c,*,1], L. Mammeri [a], H. Boucheloukh [a,b], Z. Marín [c], S. Belaidi [a], T. Sehili [a], J.A. Santaballa [c], M. Canle [c,*]

[a] Laboratoire des Sciences et Technologies de l'Environnement, Université des Frères Mentouri, Constantine 1, Constantine, Algeria
[b] Département de Chimie, Faculté des Sciences Exactes et Informatique, Université Seddik Ben Yahia, Jijel, Algeria
[c] Universidade da Coruña, React! Group, Department of Chemistry, Faculty of Sciences & CICA, E-15071 A Coruña, Spain

ARTICLE INFO

Keywords:
Propranolol
Heterogeneous photo-Fenton
Natural iron oxide
Oxalic acid
Hydroxyl radicals

ABSTRACT

We report on the degradation of aqueous propranolol (PRO) in a heterogeneous system with natural iron oxide (N.I.O.) and oxalic acid (OAA) under near UV–Vis irradiation. Photolysis experiments showed *ca.* 65% degradation of PRO after 2 h irradiation, and a similar degradation in the presence of N.I.O. A more efficient PRO removal was obtained upon irradiation within a mixture of N.I.O. and OAA. Under the best conditions considered, complete degradation (> 95%) was observed in less than 10 min, and TOC decreased by 60% after 3 h irradiation. The observed processes were adequately fitted by pseudo-first-order kinetics, the corresponding rate constants were determined, and the effect of different variables analyzed. Photodegradation of PRO is accelerated under acidic conditions, and neutralization takes place along the reaction. Hydroxyl radicals play a predominant role in the photodegradation reaction, as shown by the dramatic inhibition observed upon *t*-butanol addition. Furthermore, $HO^{\bullet}$ formation is strongly dependent on the pH of the medium. LC-MS identification of ten different intermediates leads to the proposal of a degradation mechanism. This photocatalytic system has also proven effective, for the first time, in different real aqueous matrices (river water > distilled water > sewage ≫ > seawater, revealing quite efficient in the former) and also employing sunlight, where PRO photodegradation was slower. The results obtained show that N.I.O.-oxalate complexes are a green, cheap choice for removing organic pollutants in aqueous solution.

1. Introduction

The presence of pharmaceuticals in aquatic environments and, therefore, in drinking water is of major concern due to their extensive use and incomplete removal during water treatment. [1,2] Propranolol (PRO, 1-naphthalen-1-yloxy-3-(propan-2-ylamino)propan-2-ol, Fig. 1) is a β-adrenergic blocker used for the treatment of hypertension, angina pectoris, and arrhythmia. [3] With more than 9 million prescriptions in the U.S. in 2019, [4] it is included in the WHO Model List of Essential Medicines. This drug has been repeatedly found in natural and wastewaters [5,6] at concentrations ranged from 0.07 to 89 $ng{\cdot}L^{-1}$ (median values of different studies) [7] and up to 18 $ng{\cdot}L^{-1}$ [8], respectively.

Besides, several studies have informed about the potential toxic effects of this compound, so that its presence in surface water can pose a risk to both humans and aquatic ecosystems. [9,10] PRO toxicity to different organisms has been assessed in several studies; for instance, the average 48-h LC_{50} for *Daphnia magna*, *Ceriodaphnia dubia* and *Oryzias latipes* was 1.6, 0.85 and 24.3 $mg{\cdot}L^{-1}$, respectively. [11] Thus, the development of novel technologies to efficiently remove pharmaceuticals such as β-blockers is of great importance. Several studies have indicated that advanced oxidation processes (AOPs) are able to remove β-blockers from aqueous solution. [12,13]

Photocatalysis using iron oxides is a popular technology because they are widely available and inexpensive, [14] as they comprise natural minerals abundant in the Earth's crust. [15]. Major iron oxides show semiconductor properties with a narrow band gap of 2.0–2.3 eV and, thus, they can be photoactive under solar radiation. [16] As a result, they may act as natural photocatalysts to mediate the degradation of organic pollutants in the environment. [17,18] Typically, their induced-reactions start with sunlight excitation of semiconductor particles to

* Corresponding authors.
E-mail address: moises.canle@udc.es (M. Canle).
[1] These authors contributed equally.

https://doi.org/10.1016/j.jwpe.2021.102514
Received 27 September 2021; Received in revised form 3 December 2021; Accepted 10 December 2021
Available online 6 January 2022

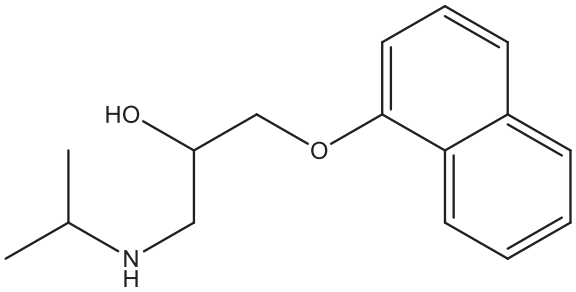

Fig. 1. Molecular structure of PRO.

produce conduction band electrons (e^-) and valence band positive holes (h^+) (Eq. 1), which may prompt photoreduction and photooxidation processes, respectively. [16,19] Thus, these excited electrons can be transferred to molecular oxygen (O_2) to form the superoxide anion ($O_2^{\bullet-}$):

$$\text{Iron oxide} + h\nu \rightarrow h^+ + e^- \quad (1)$$

$$O_2 + e^- \rightarrow O_2^{\bullet-} \quad (2)$$

Hydroxyl radicals ($HO^\bullet$) can be formed *via* oxidation of HO^- by h^+:

$$HO^- + h^+ \rightarrow HO^\bullet \quad (3)$$

The photoinduced degradation of organic pollutants by irradiated iron oxides has been extensively investigated with different degrees of success [20–24], but it has been recently found that this mode of degradation can be accelerated by photo-Fenton-like reactions assisted by polycarboxylic acids (oxalic, malic, citric, tartaric, *etc.*). [21,25–29] These carboxylic acids show an important chelating ability toward multivalent cations. [30] In particular, oxalic acid reveals quite promising as compared to similar compounds, due to its acid strength, good complexing characteristics and high reducing potential. [31] Oxalic acid ($H_2C_2O_4$, OAA) can bind iron oxide to form ≡Fe(III)-oxalate complexes through chemical adsorption (Eq. 4), where ≡ stands for the N.I.O. surface lattice. The photolysis of these complexes results in an oxidative degradation of the oxalate ligand and the reduction of the ferric center to Fe(II) (Eq. (5)), [32] a process that may also occur in solution with solubilized iron ions (Eq. (6)). Thus, a series of reactive oxygen species (ROS), such as $CO_2^{\bullet-}$, $O_2^{\bullet-}$, and $HO_2^\bullet$ (Eqs. 7, 8, and 9, respectively) are produced in the solution. Besides, H_2O_2 can be obtained by dismutation of $O_2^{\bullet-}/HO_2^\bullet$ (Eq. (10)) or *via* oxidation of Fe^{2+} (Eq. (11)). Superoxide anion can also react with Fe^{3+} yielding the ferrous cation (Eq. (12)). Fe (II) and H_2O_2 may react to produce the hydroxyl radical, $HO^\bullet$ (Fenton reaction, Eq. (13)), which acts as primary oxidant. [33–35] This radical reacts readily and unselectively with organic compounds due to its very high oxidation potential (+2.80 V *vs.* NHE). [36] Therefore, organic pollutants can be efficiently degraded, or even mineralized, in this photochemical system. Reaction (13) generates HO· in a relatively slow way, considering its reported k=40-80 $M^{-1}{\cdot}s^{-1}$ [37], and the concentrations of both Fe^{2+} and H_2O_2.

$$\text{iron oxide(s)} + nH_2C_2O_4 \rightarrow \left[\equiv Fe(C_2O_4)_n\right]^{(3-2n)} \quad (4)$$

$$\left[\equiv Fe^{III}(C_2O_4)_n\right]^{3-2n} + h\nu \rightarrow \left[\equiv Fe^{II}(C_2O_4)_{(n-1)}\right]^{4-2n} \Big/ \left[Fe^{II}(C_2O_4)_{(n-1)}\right]^{4-2n} + C_2O_4^{\bullet-} \quad (5)$$

$$Fe^{III}[C_2O_4)_n\Big]^{3-2n} + h\nu \rightarrow \left[Fe^{II}(C_2O_4)_{(n-1)}\right]^{4-2n} + C_2O_4^{\bullet-} \quad (6)$$

$$C_2O_4^{\bullet-} \rightarrow CO_2 + CO_2^{\bullet-} \quad (7)$$

$$C_2O_4^{\bullet-}/CO_2^{\bullet-} + O_2 \rightarrow 2CO_2/CO_2 + O_2^{\bullet-} \quad (8)$$

$$HO_2^\bullet + H_2O \rightleftharpoons O_2^{\bullet-} + H_3O^+ \ (pK_a = 4.8) \quad (9)$$

$$2\left(O_2^{\bullet-}/HO_2^\bullet\right) + nH^+ \rightarrow H_2O_2 + O_2 \quad (10)$$

$$O_2^{\bullet-}/HO_2^\bullet + nH^+ + Fe^{2+} \rightarrow Fe^{3+} + H_2O_2 \quad (11)$$

$$O_2^{\bullet-} + Fe^{3+} \rightarrow Fe^{2+} + O_2 \quad (12)$$

$$Fe^{2+} + H_2O_2 \rightarrow Fe^{3+} + OH^- + HO^\bullet \ \left(k = 40 - 80\ M^{-1}{\cdot}s^{-1}\right) \quad (13)$$

Though several studies are available on the photocatalytic transformation of PRO [13,38–40], its photodegradation pathways using the iron oxide-oxalate complex system have not yet been described. Besides, to the best of our knowledge, this procedure has not been tested under real conditions, *i.e.* employing sunlight and with pollutants dissolved in complex matrices, rather than distilled water. This last point is very important to assess the feasibility of this technique. In fact, the major objective of this study was the evaluation of the system comprised of suspended natural iron oxide (N.I.O.) together with OAA to photodegrade PRO, as a model pollutant in water, with no other chemicals added to obtain a very efficient, economical, sustainable technique for water decontamination. The effect of OAA concentration, N.I.O. load, and pH on the photodegradation was analyzed. The degree of pollutant mineralization was also examined, and the efficiency of the reaction was tested in different aqueous matrices and using solar radiation. Besides, products and intermediates of the photocatalytic degradation of PRO have been identified and appropriate reaction pathways proposed.

2. Materials and methods

2.1. Materials

Overall, reactants of the highest purity commercially available were used. (±)-propranolol hydrochloride (≥99%, Sigma-Aldrich), oxalic acid 2-hydrate (PRS, Panreac), sodium hydroxide (PA-ACS-ISO, Panreac), 1,10 phenanthroline monohydrate (p.a., Merck), sodium acetate (99%, Panreac), sulfuric acid (96% p.a., Panreac), titanium tetrachloride (98%, Fluka), potassium dihydrogen phosphate (p.a., Merck), phosphoric acid (85% RPE-ACS, Carlo Erba), and acetonitrile (Ultra Gradient HPLC Grade, J. T. Baker) were employed in the experiments, without further purification. Natural iron oxide (N.I.O.) was obtained from Châabet El Ballout mine in Souk Ahras, NE Algeria, ground and used without any chemical treatment. N.I.O. has already been characterized by X-ray powder diffraction (XRD), X-ray fluorescence, energy-dispersive X-ray spectroscopy (EDX), Brunauer-Emmett-Teller (BET) surface area measurement, scanning electron microscopy (SEM), and Raman spectroscopy in previous studies. [41,42] Particle size distribution has been analyzed with a Saturn Digisizer II laser granulometer and the density measured with an Accupyc 1340 helium pycnometer, both from Micromeritics, Inc.

According to EDX (Table 1) N.I.O. contains mostly iron (50%) and

Table 1
most abundant elements present in N.I.O. as analyzed by EDX. [41].

Element	Fe	O	C	Ca	Si	Mn	Al
% (weight)	50 ± 3	38 ± 2	7.4 ± 2.3	2.1 ± 0.3	1.5 ± 0.1	1.5 ± 0.3	0.5 ± 0.1

oxygen (38%), with smaller amounts of carbon, calcium, silicon, manganese, and aluminum. XRD data confirmed that it is mostly composed of hematite, the alpha polymorph of Fe_2O_3. [41] Particle size distribution is broad, where particles with diameter ranging 0.2–100 μm comprise 99% of the total volume, with a mean value of 20.6 μm, median of 14.2 μm, and mode is 23.8 μm. These particles present different morphologies according to SEM micrographs: N.I.O. mostly contains irregular micrometric particles in the form of aggregates and some small spherical particles. [41] This corresponds to a BET specific surface area, measured by N_2 adsorption, of 79 $m^2 \cdot g^{-1}$, and a total pore volume of 0.0892 $cm^3 \cdot g^{-1}$. The density of this material is relatively high for a clay, 3.856 $g \cdot cm^{-3}$.

All solutions were prepared with bidistilled, organic matter-free water, whereas Millipore Milli-Q® ultrapure water (resistivity ≥18.2 MΩ·cm) was employed as HPLC mobile phase.

2.2. Photodegradation experiments

Irradiation experiments were carried out in a stirred batch photoreactor, comprising a 200 mL borosilicate glass photoreactor and an ultraviolet A plus visible (UVA–Vis) light source (Fig. 2). A Heraeus medium-pressure mercury-vapor lamp, model TQ-150-Z3, is cooled to 298.0 ± 0.1 K by water circulation, and irradiation bands below 350 nm were cut off with a Duran 50® glass filter. The photoreactor was covered with aluminum foil to reflect escaping radiation and to avoid the entrance of any other light; thus, photon flux at 366 nm was $2.38 \cdot 10^{-6}$ Einstein·s^{-1}.

Continuously stirred suspensions, formed by adding the desired quantity of N.I.O. powder into 200 mL of PRO and OAA aqueous solution, were kept in the dark for 30 min to allow for the adsorption-desorption equilibrium to be established. Initial PRO concentration was 8 ppm in all experiments, far below PRO solubility in water at 298 K (61.7 ppm), [43] and pH was not adjusted unless stated otherwise, thus resulting in the natural pH of the heterogeneous mixture. Photodegradation experiments were initiated by insertion of the previously warmed up lamp (15 min) and then, samples were collected at specific times, filtered through 0.45 μm Sartorius nylon filters, to remove particles, and analyzed. It was previously checked that the nylon filters did not retain PRO to a measurable level, and consequently assumed the same was true for PRO metabolites.

For solar experiments, magnetically stirred borosilicate flasks were placed under sunlight with a 100 mL suspension of PRO, OAA and N.I.O., and the same procedure was followed.

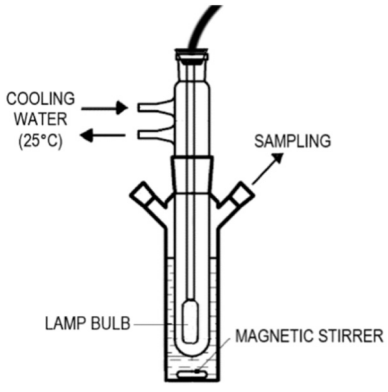

Fig. 2. Schematic representation of the stirred batch photoreactor employed in the study.

2.3. Analytical methods

2.3.1. HPLC analysis

Filtered samples were analyzed with a Thermo Finnigan HPLC instrument equipped with a diode-array UV–Visible detector and a Scharlau KromaPhase 100 C18 column (5 μm, 250 × 4.6 mm). A 35:65 mixture of acetonitrile and pH 2.5 buffer (0.01 M KH_2PO_4/H_3PO_4) at a flow rate of 1.0 mL·min^{-1} was used as mobile phase, and PRO was detected at 289 nm.

2.3.2. UHPLC-MS analysis

The identification of obtained photoproducts was carried out by UHPLC-MS, using a Thermo Fisher Scientific LTQ-Orbitrap Discovery mass spectrometer, equipped with an electrospray interface operating in positive ion mode (ESI+), coupled to a Thermo Fisher Scientific Accela UHPLC apparatus. A Phenomenex Kinetex XB-C18 column (2.6 μm, 100 × 2.1 mm) column was used. Analyses were carried out using full-scan data-dependent MS, acquiring data from m/z = 50 to 400.

2.3.3. Other analytical measurements

Total organic carbon (TOC) values were measured in a Shimadzu TOC 5000A analyzer. Results at different reaction times were compared to the starting value to determine the mineralization degree. [Fe^{2+}] in solution was measured by the 1,10-phenanthroline method. [44] [H_2O_2] was measured using a colorimetric method based on its derivatization with $TiCl_4$ reagent, where the molar absorption coefficient at 410 nm is $\varepsilon = 720\ M^{-1} \cdot cm^{-1}$. [45]

2.4. Recovery of the catalyst

N.I.O. was recovered after its use following a very simple procedure. The nylon filter employed during the experiment was backwashed with distilled water and this effluent, containing some N.I.O., was merged with the leftover reaction solution and, therefore, with the remaining

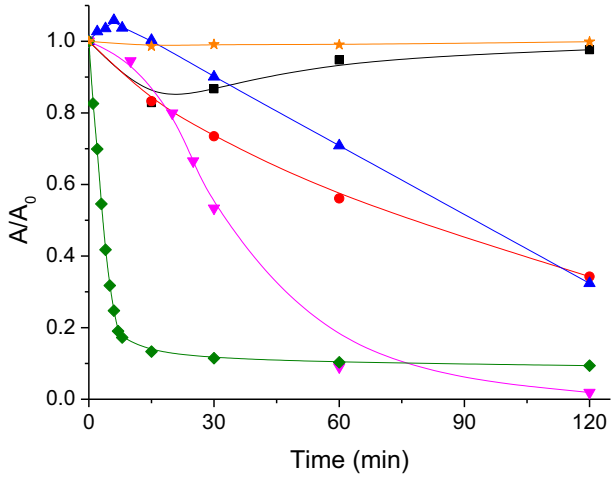

Fig. 3. Degradation of 8 ppm PRO under different conditions: (■) 1.0 g·L^{-1} N.I.O., (★) 1.0 mM OAA, (●) UVA–Vis, (▲) 1.0 g·L^{-1} N.I.O. + UVA–Vis, (▼) 1.0 mM OAA + UVA–Vis, and (♦) 1.0 g·L^{-1} N.I.O. + 1.0 mM OAA + UVA–Vis. T = 298 K, $pH_{(PRO)}$ = 7.2, $pH_{(PRO+N.I.O.)}$ = 9.3, $pH_{(PRO+OAA)}$ = 3.2, $pH_{(PRO+N.I.O.\ +\ OAA)}$ = 4.2.

catalyst. The particles of N.I.O. were allowed to settle for 2 h, the supernatant was decanted away, and the sediment was dried in the same reaction vessel at 90 °C for 12 h, prior to the following degradation run. No washing or any other further treatment of the used N.I.O. was performed.

3. Results and discussion

PRO degradation in aqueous solution under different reaction conditions, presence and absence of N.I.O. and/or OAA, and either in the dark or under UVA–Vis irradiation, is shown in Fig. 3. In this and the following figures, unless differently stated, lines just represent tendencies and are not mathematical fits of mechanistic models.

PRO does not decrease within 2 h in the dark; the addition of N.I.O. did not induce degradation, but some weak surface interaction phenomena in the heterogeneous medium at natural pH. Also, no effect was observed with OAA alone. Therefore, no evidence of significant adsorption or degradation of PRO has been observed in the dark. PRO is a weak base with $pK_a = 9.5$ [46] and N.I.O has zeta potential >0 when 2 < pH < 8). [47,48]

The fact that both PRO and N.I.O. are positively charged at pH < 9 explain the lack of PRO adsorption onto N.I.O. On the other hand, approximately 65% conversion was observed with or without N.I.O. after 2 h of lamp irradiation, indicating a relatively slow photolysis process and the absence of any relevant effect of N.I.O. Light dispersion by N.I.O. suspended particles accounts for the difference between UVA–Vis and N.I.O. + UVA–Vis experiments. This suggests that the photoreductive dissolution of N.I.O. does not present any noticeable effect on PRO degradation, [49,50] and that the photocatalytic activity of N.I.O. particles acting as a semiconductor (generation of e^-/h^+ pairs) has a minor contribution under these conditions, despite it has been previously observed in other systems. [17,18]

OAA/UVA–Vis system leads to a 98% degradation of PRO in 2 h. This is attributed to H_2O_2 production by the direct photolysis of OAA to yield $HO^\bullet$. [51] When 1.0 g·L^{-1} N.I.O. was added to the reaction medium, the degradation notably accelerated by the photo-Fenton-like system, and the reaction took place in *ca.* 15 min, with 80% PRO elimination. Degradation of PRO under suitable conditions is adequately fitted by a first-order kinetic model, and the corresponding rate constants (k) are listed in Table 2.

Table 2
First-order kinetic rate constants (k) obtained for the photodegradation of 8 ppm PRO under different initial conditions. All experiments performed with distilled water. $T = 298$ K.

Radiation	[N.I.O.]/ g·L^{-1}	[OAA]/ mM	[*t*-BuOH]/ mM	pH	k·10^6/s^{-1}
None	1.0	–	–	9.3 (natural)	12 ± 13
None	–	1.0	–	3.2 (natural)	1 ± 1
Lamp	–	–	–	7.2 (natural)	159 ± 7
Lamp	–	–	0.1	7.2 (natural)	55 ± 3
Lamp	1.0	–	–	9.3 (natural)	112 ± 19
Lamp	–	1.0	–	3.2 (natural)	348 ± 60
Lamp	0.5	1.0	–	3.4 (natural)	6198 ± 318
Lamp	1.0	1.0	–	4.2 (natural)	3565 ± 243
Lamp	1.0	1.0	0.1	4.2 (natural)	61 ± 5
Lamp	2.0	1.0	–	6.9 (natural)	130 ± 15
Lamp	1.0	0.5	–	5.7 (natural)	92 ± 8
Lamp	1.0	2.0	–	3.0 (natural)	6158 ± 515
Lamp	1.0	1.0	–	4.8	1938 ± 142
Lamp	1.0	1.0	–	10.5	79 ± 41

As already observed for other compounds, [52] PRO photodegradation must take place both on the iron oxide surface (heterogeneous process) and in solution (homogeneous reaction). Once N.I.O. is added to the solution, OAA is chemically adsorbed on N.I.O. surface forming iron oxide–oxalate complexes ($[\equiv Fe^{III}(C_2O_4)_n]^{3-2n}$). Zeta potential becomes negative at pH *ca.* 2. [48] The N.I.O.-oxalate system under UVA–Vis irradiation can be excited to yield radicals such as $C_2O_4^{\bullet-}$, $CO_2^{\bullet-}$, $O_2^{\bullet-}/HO_2^\bullet$ and $HO^\bullet$ (Eqs. (5)–(9) & (13)). The hydroxyl radical ($HO^\bullet$) is an extremely strong, non-selective oxidant leading to the mineralization of most organic chemicals. Iron(III)-oxalate complexes ($[Fe^{III}(C_2O_4)_n]^{3-2n}$), $Fe^{2+}$and H_2O_2 are also formed in solution: the two latter react to produce $HO^\bullet$ radicals (Eq. (13)), while the photolysis of Fe(III)-oxalate complexes in solution yields $HO^\bullet$ as well. Additional ROS, such as radical cations, arise from photodegradation of OAA and, though it is dependent on N.I.O. nature, $k = 3.5{\cdot}10^{-2}$ min^{-1} may be accepted for the corresponding rate constant (Eq. (14)). [52,53]

$$OAA + O_2 + h\nu \rightarrow OAA^{\bullet+} + O_2^{\bullet-} \quad (14)$$

Finally, photoinduced homolysis of H_2O_2 also leads to formation of $HO^\bullet$ radicals (Eq. (15)).

$$H_2O_2 + h\nu \rightarrow 2\ HO^\bullet\ (\lambda \leq 365\ nm) \quad (15)$$

3.1. Formation of H_2O_2 and Fe^{2+}

$[Fe^{2+}]$ and $[H_2O_2]$ in solution, both involved in Fenton reaction, were monitored (Fig. (4)). H_2O_2 is generated *via* two pathways: $HO_2^\bullet$ reacting with $O_2^{\bullet-}/HO_2^\bullet$ (Eq. (10)) and Fe(II) reacting with $O_2^{\bullet-}/HO_2^\bullet$ (Eq. (11)). In the described experiment, *i.e.* 1.0 g·L^{-1} N.I.O., 1.0 mM OAA, and UVA–Vis lamp, $[H_2O_2]$ reaches a maximum value of $3.6{\cdot}10^{-4}$ M after 10 min. This photochemical reaction occurs both onto the iron oxide surface and also in the bulk of the solution. [49,52] In the course of photodissolution of N.I.O., dissolved iron may be photoreduced to Fe^{2+}, reaching a peak value of $2.9{\cdot}10^{-5}$ M after 15 min. Fe(II) formation profile is similar to that occurring with goethite, where two stages have been identified, the first one is slower and then the presence of Fe(II) speeds up the process. [54] $[Fe^{2+}]$ and $[H_2O_2]$ in Fe(III) + oxalate systems show different profiles depending on the medium pH, $[Fe(III)]_0$ and $[\text{oxalate ion}]_0$, [33,48,55] but it is also conditional on the incident radiation. The presence of ferrous cations is the determining-step for the overall reaction rate. However, it has been reported that both the lack and the excess of iron cations (both Fe^{2+} and Fe^{3+}) are not favorable for the degradation of organic pollutants. [56] Thus, iron leaching is crucial

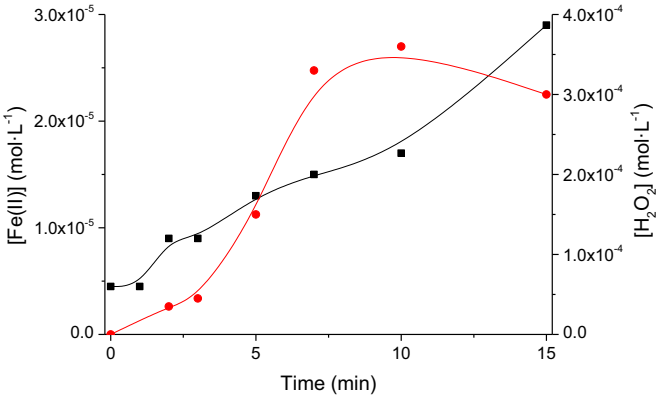

Fig. 4. Formation of Fe^{2+} (■) and H_2O_2 (●) during the photodegradation of 8 ppm PRO under UVA irradiation in the presence of 1.0 g·L^{-1} N.I.O. and 1.0 mM OAA $T = 298$ K, pH = 4.2.

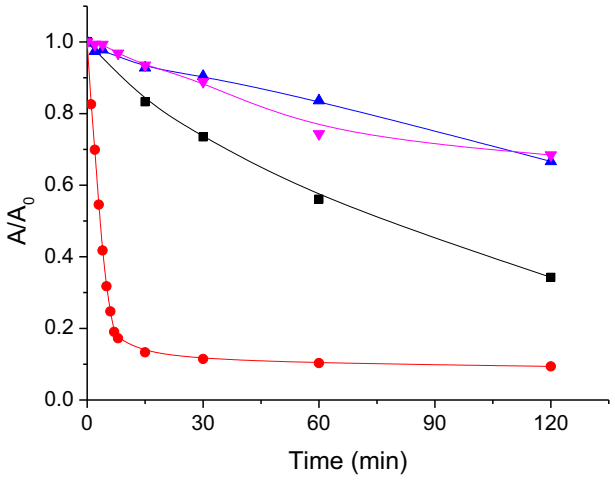

Fig. 5. Effect of 0.1 mM *t*-butanol on the photodegradation of 8 ppm PRO: (■) only UVA–Vis irradiation; (●) UVA–Vis irradiation with 1.0 g·L^{-1} N.I.O. + 1.0 mM OAA; (▲) UVA–Vis irradiation with 0.1 mM *t*-BuOH; (▼) UVA–Vis irradiation with 1.0 g·L^{-1} N.I.O. + 1.0 mM OAA + 0.1 mM *t*-BuOH. T = 298 K, $pH_{(PRO)}$ = 7.2, $pH_{(PRO+N.I.O. + OAA)}$ = 4.2.

in the catalytic process (more information below, in Section 3.4).

3.2. Effect of tert-butanol

t-BuOH is a commonly used HO$^{\bullet}$ scavenger, [20] as the corresponding reaction rate is very fast ($k_{(HO^{\bullet} + t\text{-BuOH})}$ = 6.0·10^8 M^{-1}·s^{-1}) [36] and the resulting radical is relatively inert. It has been observed that small amounts of *t*-BuOH (0.1 mM) inhibited *ca.* 60% of the photocatalytic degradation of PRO in 2 h (Fig. 5). Besides, PRO direct photolysis was similarly affected by *t*-BuOH, exhibiting kinetics that are comparable to the inhibited photo-Fenton-like process. This indicates that HO$^{\bullet}$ is also generated during PRO photolysis, which must be attributed to PRO acting as a photosensitizer. [57,58] The comparison between the effect of *t*-BuOH on PRO direct photolysis and photocatalysis (Fig. 5) suggests that PRO removal by N.I.O. + OAA photocatalysis is mainly promoted by HO$^{\bullet}$.

Competition between oxalate and PRO by HO$^{\bullet}$ could be discarded, since $k_{(PRO+HO^{\bullet})}$ is diffusion controlled [59] whereas $k_{(HO^{\bullet} + oxalate)}$ = 10^7 M^{-1}·s^{-1}. [60]

3.3. Effect of photocatalyst concentration

The catalyst load may have a positive or negative impact on the photodegradation depending on its amount. An increase in photocatalyst concentration means a higher number of reactive sites, thus increasing the degradation rate. On the other hand, the addition of an excess of catalyst increases turbidity and light dispersion, reducing the amount of effective UV photons, which negatively affects the reaction rate. Besides, N.I.O. also has some effect on the pH of the reaction medium, as it increases with catalyst concentration, which decreases the degradation rate (see below, Section 3.5). We have tested all these factors together, by modifying the amount of catalyst without changing the other chemicals that participate in the reaction. Thus, to determine the optimal N.I.O. dosage, experiments were carried out in the 0.5–2.0 g·L^{-1} N.I.O. range, while PRO was kept constant and pH was not adjusted (Fig. 6). The obtained results indicate that photodegradation efficiency increases with decreasing N.I.O. load. First-order kinetic rate constants (k) are listed in Table 2.

More Fe(III)-oxalate complexes may be formed on the surface or in solution with growing N.I.O. load, and consequently, more HO$^{\bullet}$ should be produced, and increased PRO degradation would be expected. [61] However, a degradation decrease is observed at higher catalyst loads, which is attributed to strong light dispersion by suspended particles, that reduces the availability of photons and, therefore, the formation of HO$^{\bullet}$. Also, the increase in pH with growing [N.I.O.] (see Section 3.5) operates against the photodegradation process.

3.4. Effect of oxalic acid concentration

[OAA]$_0$ is an important factor to determine optimal PRO-removal conditions. This effect was investigated from 0.5 to 2.0 mM OAA at constant 1 g·L^{-1} N.I.O. load (Fig. 7). PRO photodegradation has proved very sensitive to oxalate, its efficiency increases with [OAA]$_0$. As it increases, both adsorbed and in solution Fe(III)-oxalate complexes also increase and, consequently, the amount of reactive radical species responsible of PRO degradation. Besides, a higher amount of OAA leads to a more acidic initial pH, which also markedly affects the reaction rate (Section 3.5).

pH changes along the reaction, increasing with time (Fig. 8), so that the initial acid pH of the medium is mostly neutralized by the end of the reaction. This implies an important advantage for this system with respect to regular photo-Fenton processes using H_2O_2 in acidic medium, as any subsequent neutralization steps may not be necessary. This change can be explained by the consumption of OAA (Eqs. (1)–(9) [52]

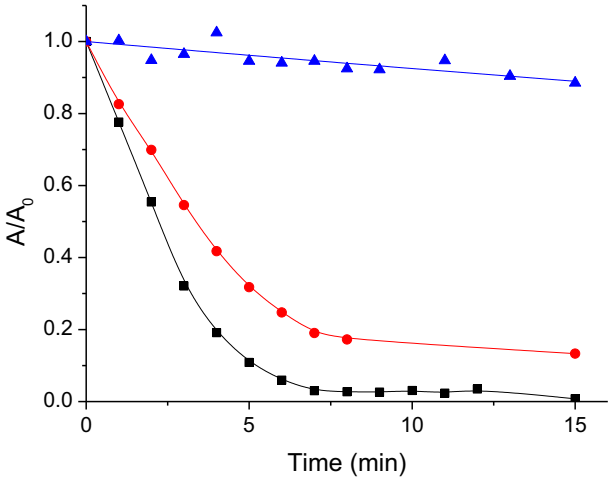

Fig. 6. N.I.O. dosage effect on the photodegradation of 8 ppm PRO under UVA–Vis irradiation in the presence of 1.0 mM OAA [N.I.O.] = 0.5 g·L^{-1} (■, pH = 3.4); 1.0 g·L^{-1} (●, pH = 4.2); or 2.0 g·L^{-1} (▲, pH = 6.9). T = 298 K.

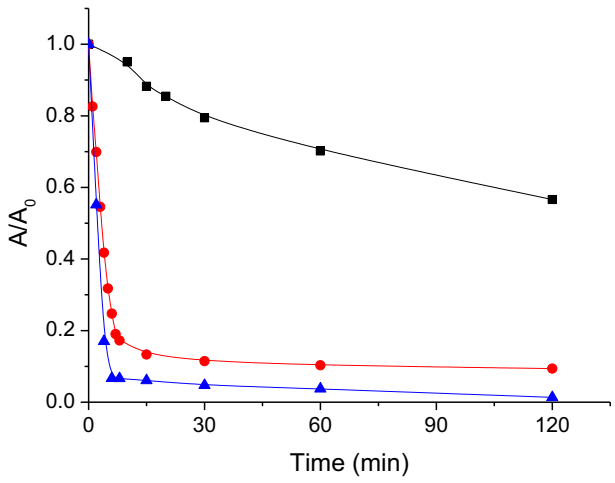

Fig. 7. Effect of initial OAA concentration on PRO photodegradation under UVA–Vis irradiation with [PRO] = 8 ppm, [N.I.O.] = 1 g·L^{-1}, and [OAA] = 0.5 mM (■, pH = 5.7); 1.0 mM (●, pH = 4.2); or 2.0 mM (▲, pH = 3.0). T = 298 K.

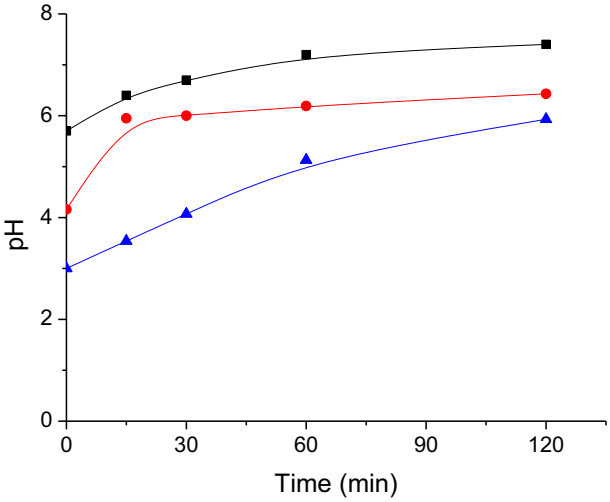

Fig. 8. pH variation along the photodegradation of 8 ppm PRO under UVA–Vis irradiation, with 1 g·L^{-1} N.I.O. and different values of initial OAA concentration: [OAA] = 0.5 mM (■), 1.0 mM (●), or 2.0 mM (▲). T = 298 K.

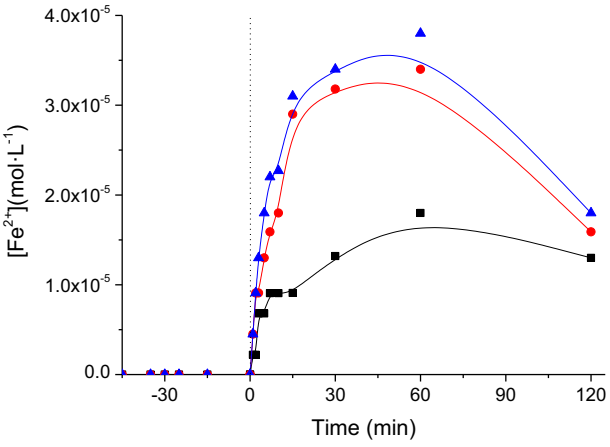

Fig. 9. Concentration of Fe^{2+} along the photodegradation of 8 ppm PRO under UVA–Vis irradiation, with 1 g·L^{-1} N.I.O. and different values of initial OAA concentration: [OAA] = 0.5 mM (■), 1.0 mM (●), or 2.0 mM (▲). Initial 45 min correspond to the period in the dark for the establishment of the adsorption equilibria. T = 298 K.

along with HO$^{\bullet}$ production (Eq. (13)), with a minor contribution of HO^- generation, and H_2O_2 formation, which also consumes protons (Eqs. (10) & (11)).

Iron leaching depends on the concentration of OAA and the processes undergone are strongly affected by the irradiation (Fig. 9). An increase in OAA led to a rise in [Fe^{2+}] under irradiation, whereas the presence of this cation in the reaction medium was negligible in the dark. It has been reported that iron oxides can be quickly dissolved in OAA solution, but the reduction process of Fe^{3+} hardly occurs without irradiation. [35] Besides, the dissolution of iron oxides in organic acid solutions is promoted by ultraviolet and visible light radiation (Eqs. (5) & (6)) [26,33]. [Fe^{2+}] increases along the first 60 min of irradiation as Fe(III)-oxalate complexes are easily photodissolved and reduced to Fe(II)-oxalate complexes (Eq. (6)); [62] Fe^{2+} ions can be also produced through Eq. (12). In the late stage of the reaction, the transference of iron cations

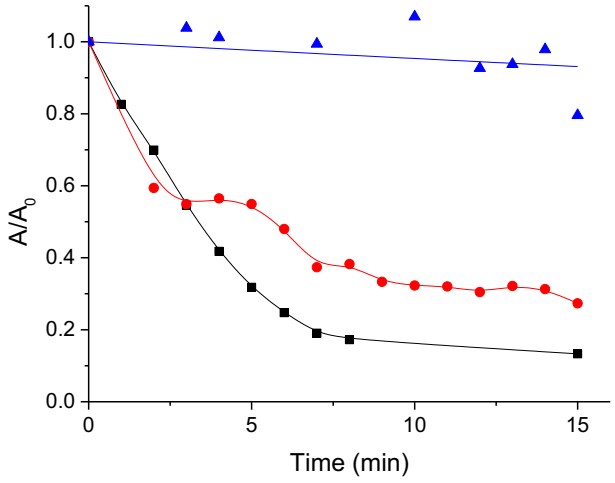

Fig. 10. Effect of initial pH on the photodegradation of 8 ppm PRO in the presence of N.I.O. (1 g·L^{-1}) and OAA (1.0 mM) under UVA–Vis irradiation. pH = 4.2 (■), 4.8 (●), or 10.5 (▲). T = 298 K.

from the N.I.O. surface to the solution slows down due to both the consumption of OAA and the corresponding pH increase. Under these conditions, Fe^{3+} precipitates as $Fe(OH)_3$ so that the concentration of Fe^{3+} declines. [35]

3.5. Effect of initial pH

pH is commonly an essential parameter for photo-Fenton processes. In this study we have employed natural pH after the addition of the necessary OAA, for avoiding the use of other chemicals. Still, we have also checked the effect of this parameter on the kinetics of the degradation process. Photocatalytic degradation of PRO was examined at pH values 4.2, 4.8, and 10.5 by adjusting pH with NaOH(aq) (Fig. 10). The best results were obtained under acidic conditions (pH 4.2), where dissolved Fe must be present predominantly as the photoactive $[Fe^{III}(C_2O_4)_3]^{3-}$ and $[Fe^{II}(C_2O_4)_2]^{2-}$ complexes. [63] This result is in agreement with the previously reported optimal pH range around 3–4 for the photodegradation of organic pollutants in the N.I.O.-oxalate complex system. [20,42] At higher pH (4–5) predominant Fe(III)-oxalate complexes are less photoactive, [49,52] thus PRO photodegradation at pH 4.8 is slowed down.

A negligible decrease in PRO concentration at pH 10.5 was observed. Under alkaline conditions the predominant Fe(III)/Fe(II) species are the insoluble hydroxides $Fe(OH)_3$ and $Fe(OH)_2$ that readily precipitate. Therefore, the generation of active species is strongly inhibited at basic pH values, preventing PRO photodegradation.

3.6. Photodegradation products and proposed reaction pathways

The main transformation products formed during UVA–Vis irradiation of PRO in the N.I.O.-oxalate system were identified by HPLC-MS, in positive ion mode, and are summarized in Table 3. The m/z value of each peak corresponds to the molecular ion $[M + H]^+$. Some of them have been also previously reported as intermediates of different oxidation processes of PRO [64–68] Propranolol contains two types of reactive sites, the aromatic moiety and the lateral chain (Fig. 1). Under attack of HO$^{\bullet}$, C—O bond breaking takes place, releasing the lateral group. [64] Piram et al. studied the photochemical behavior of PRO in environmental waters; [69] they observed hydroxylation only in the aromatic

Table 3
Intermediates detected in PRO photodegradation by HPLC/MS, in positive ion mode.

	Name	m/z	t_R (min)	Proposed structure
PRO	Propranolol ($C_{16}H_{21}NO_2$)	260.1645	12.24	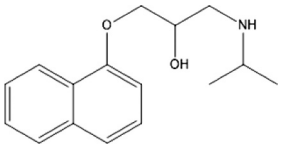
P1	Naphthol ($C_{10}H_8O$)	145.0648	12.27	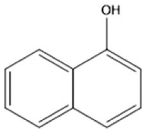
P2	3-(Isopropylamino)propane-1,2-diol ($C_6H_{15}NO_2$)	134.1103	3.73	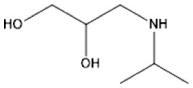
P3	Naphthoxy methanoic acid ($C_{11}H_8O_3$)	189.0648	10.44	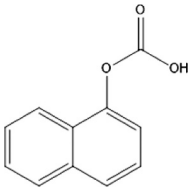
P4	2-(Isopropylamino)ethanol ($C_5H_{13}NO$)	104.1070	4.09	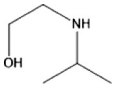
P5	Naphthalene ($C_{10}H_8$)	129.0699	12.32	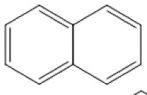
P6	8-(3-(Ethylamino)-2-hydroxypropoxy)naphthalen-1-ol ($C_{15}H_{19}NO_3$)	262.1438	10.46	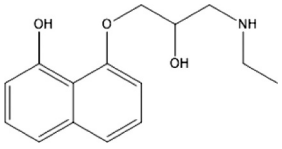
P7	(Z)-2-(2-Hydroxy-3-(isopropylamino)propoxy)-6-(2-hydroxyethylidene)cyclohexa-2,4-dienone ($C_{14}H_{21}NO_4$)	268.0816	12.73	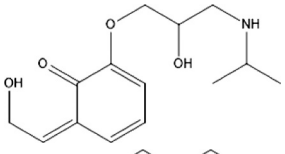
P8	(Z)-2-(5-(2-Hydroxy-3-(isopropylamino)propoxy)-6-oxocyclohexa-2,4-dienylidene)acetaldehyde ($C_{14}H_{19}NO_4$)	266.1314	10.64	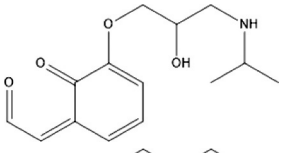
P9	(Z)-2-(5-(3-Amino-2-hydroxypropoxy)-6-oxocyclohexa-2,4-dienylidene)acetaldehyde ($C_{11}H_{13}NO_4$)	224.0917	10.51	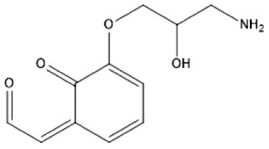
P10	1-((5Z,6E)-6-Ethylidene-5-(hydroxymethylene)cyclohexa-1,3-dienyloxy)-3-(isopropylamino)propan-2-ol ($C_{14}H_{17}NO_4$)	264.1230	10.30	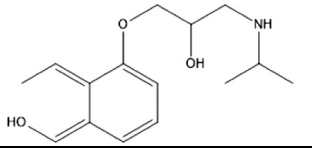

On the basis of the above reported results and taking into account the information reported in the literature, [64,66,67] the following PRO degradation pathways are proposed (Scheme 1).

moiety without hydroxylation of the lateral chain, in agreement with our findings.

$HO^{\bullet}$ radicals produced from the photolysis of N.I.O.-oxalate complex are responsible for the transformation of PRO by attacking this compound in the following ways:

$HO^{\bullet}$ attack takes place in the benzene ring of PRO, leading to naphthol (P_1, $m/z = 145$) with release of the lateral group, yielding the corresponding 3-(isopropylamino)propane-1,2-diol (P_2, $m/z = 134$), which have been also detected by Santiago et al. [64] and Xie et al. [70]

Further oxidation of PRO can give naphthoxy methanoic acid (P_3, $m/z = 189$). This can be justified by the presence of the fragment $C_5H_{13}NO$ (P_4, $m/z = 104$) that corresponds to a C_{11}-C_{12} bond cleavage on the side chain. Product ions at $m/z = 129$ correspond to a cleavage in the aliphatic chain of PRO leading to naphthalene (P_5).

P_6 with m/z = 262 was obtained by, firstly, the addition of $HO^•$ radicals on the aromatic ring and, secondly, the loss of one methyl group in the isopropyl moiety, followed by protonation.

The dihydroxylation of the aromatic ring led to non-observed products (m/z = 296). This was followed by an oxidative ring-opening reaction involving decarboxylation, which leads to P_7 with m/z = 268. [67] Subsequent oxidation of the alcohol moiety to aldehyde results in the formation of P_8 (m/z = 266). [67] The latter also led to the formation of P_9 (m/z = 224), the loss of 42 Da indicates the cleavage of the isopropyl group. The formation of products P_7 and P_8 has been previously observed in oxidation-coagulation treatment with ferrate ($K_2Fe^{IV}O_4$) by Wilde et al. [67]

Further, P_{10} (m/z = 264) was formed during the direct photolysis of propranolol in aqueous solution. This fragment ion was found by Qin-Tao et al. [66] who studied the degradation of propranolol by radiation in the 295–800 nm range.

3.7. Mineralization

H. Yang et al. reported that PRO was fully mineralized to CO_2 and NH_4^+, after 4 h of irradiation in the TiO_2-catalyzed photodegradation. [71] We have monitored total organic carbon (TOC) along the photocatalytic degradation of 8 ppm PRO with N.I.O. (1 $g{\cdot}L^{-1}$) and OAA (1 mM). Results showed that TOC decreases much more slowly than PRO itself, and that mineralization is far for completion after 3 h irradiation (Fig. 11). This can be explained by a multistep degradation of PRO, with formation of several organic intermediates (in agreement with the proposed reaction pathways, Scheme 1), which appear to be more resistant to photodegradation.

The observed partial mineralization of propranolol brings attention to the remaining toxicity of the incompletely degraded mixture. It has been proposed that the photodegradation products from PRO should be less toxic because of their presumed higher polarity and hydrophilicity than the parent compound, and this hypothesis has been tested in different studies. The toxicity evaluation of PRO and its degradation products by algae (*Raphidocelis subcapitata*) and rotifer (*Brachionus calyciflorus*) screening tests supported this postulate. [72] However, the toxicity to *Daphnia magna* increased during the early stages of the photocatalytic decomposition of PRO and then progressively decreased upon the elimination of this compound. [73] Also, the product mixtures obtained from PRO degradation by UV/persulfate treatment showed lower toxicity to *Vibrio fischeri* than the corresponding initial solutions. [74]

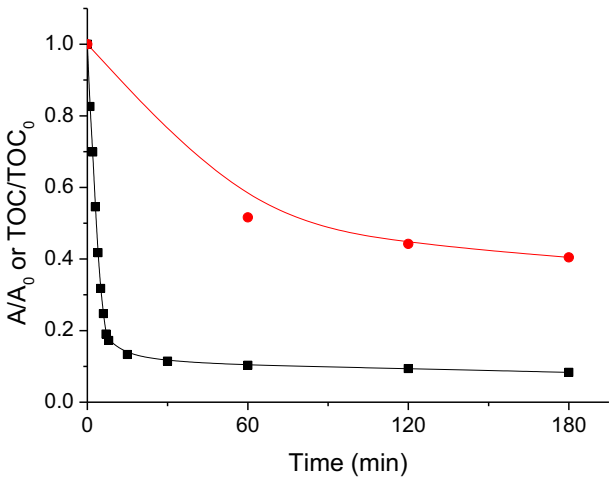

Fig. 11. Fade of initial pollutant (■) and TOC of the solution (●) in the photocatalytic degradation of 8 ppm PRO with 1 $g{\cdot}L^{-1}$ N.I.O. and 1 mM OAA under UVA–Vis irradiation. T = 298 K, pH = 4.2.

3.8. Propranolol photodegradation by N.I.O.-oxalate system under real conditions

In what has been described so far, the model pollutant, PRO, was dissolved in distilled water, and the photodegradation process occurred upon UVA–Vis irradiation with a medium pressure Hg-vapor lamp. However, the study of elimination of persistent pollutants with AOPs is intended for its application in water treatment, where these compounds are part of a complex matrix containing a number of other substances. In this context, the use of UVA (or Vis) radiation shows a relevant and sustainable advantage, as emitting lamps can be replaced by sunlight.

Taking this into account, in addition to distilled water, the elimination of PRO in sewage, river water, and seawater has been studied with UVA–Vis radiation (Fig. 12 and Table 4). The experiment was performed under the most favorable conditions among those observed in distilled water (see above), *i.e.* 1.0 $g{\cdot}L^{-1}$ N.I.O. and 2.0 mM OAA The optimal conditions were obtained with for 0.5 $g{\cdot}L^{-1}$ N.I.O. (plus 1.0 mM OAA, Fig. 6) and 2.0 mM OAA (plus 1.0 $g{\cdot}L^{-1}$ N.I.O., Fig. 7) in distilled water. However, complex matrices contain organic matter and inorganic ions. Organic matter may react with $HO^•$ radicals, consuming a higher amount of OAA, while inorganic ions may interact with N.I.O., being adsorbed on its surface and thus reducing the availability of OAA to produce ≡Fe(III)-oxalate complexes. Considering this, and to avoid any shortage of OAA that may hinder the reaction or reduce the activity, we decided to use 2.0 mM OAA and 1.0 $g{\cdot}L^{-1}$ N.I.O. for the experiments.

PRO photodegradation in sewage yielded a slower kinetic constant, which we attribute to the high concentration of organic matter in the matrix, leading to competitive reactions that consume $HO^•$. Still, the degradation of PRO was hardly affected with respect to distilled water.

The process in river water was slightly faster than in distilled water, presumably due to the presence of dissolved photosensitizing organic materials and some inorganic ions. It has been reported that humic and fulvic acids may act as natural photosensitizers. [75,76] Also inorganic ions, such as nitrate and nitrite anions may produce $NO_3^•$ and, ultimately, $HO^•$. [77] On the other hand, inorganic ions may slow down PRO photodegradation, as some of (the most effective) $HO^•$ radicals are consumed in parallel processes. [58,59]

PRO photodegradation was much slower in seawater. The presence of high concentrations of Cl^- in the matrix inhibits the reaction through two different pathways: Cl^- scavenges $HO^•$, particularly at acidic pH values, to yield the much less oxidant and less reactive species $Cl_2^{•-}$, [78] and $HO^•$ production is affected by competitive Cl^- adsorption [79] onto N.I.O. surface and by the formation of chloro-Fe(III) complexes, which photolyze to $Cl_2^{•-}$. [80] A similar analysis applies to sulfate anions. [80]

Experiments with the same aqueous matrices were also performed under sunlight (Fig. 13 and Table 4). Observed degradation rates are considerably slower than with the UVA–Vis lamp due to the lower amount of high energy photons reaching the photocatalytic system in this case.

Again, river water enhances the process with respect to distilled water, while sewage slightly reduces its rate, and it is strongly inhibited in seawater, where the process revealed quite inefficient (less than 20% degradation in 2 h). The experiments were performed in December at the Northern Hemisphere (43°19′36″ N), very close to winter solstice, when solar elevation angle is the lowest, which explains the slow degradation observed compared to artificial UVA–Vis experiments. A relevant outcome in this case is the fact that, though photodegradation with direct solar light is slower, *ca.* four times, than with the lamp, still more than 95% of PRO degradation was achieved within 30 min in river water and sewage, although such a percentage was not obtained in distilled water even after 2 h irradiation. Considering these particular conditions, the photocatalytic system here studied revealed quite adequate for the photodegradation of organic pollutants with solar radiation in several aqueous matrices, although it seems not suitable for application in seawater.

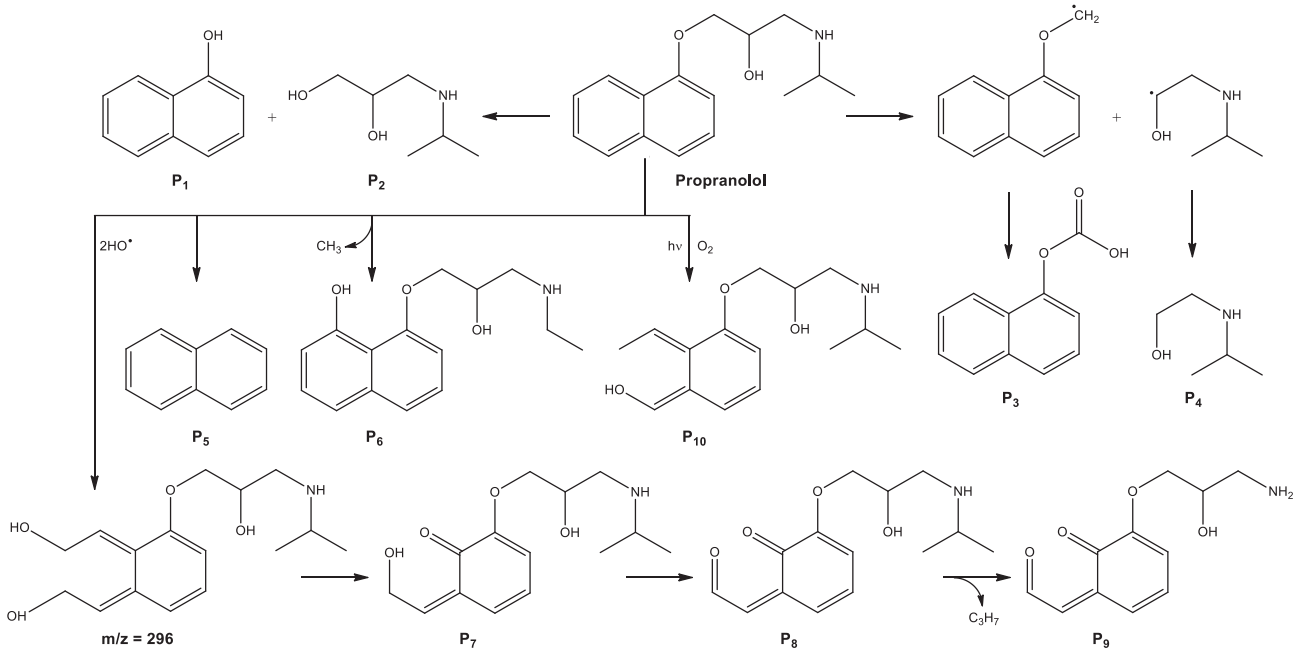

Scheme 1. Proposed degradation pathways for PRO in Fe(III)-oxalate / UVA–Vis systems.

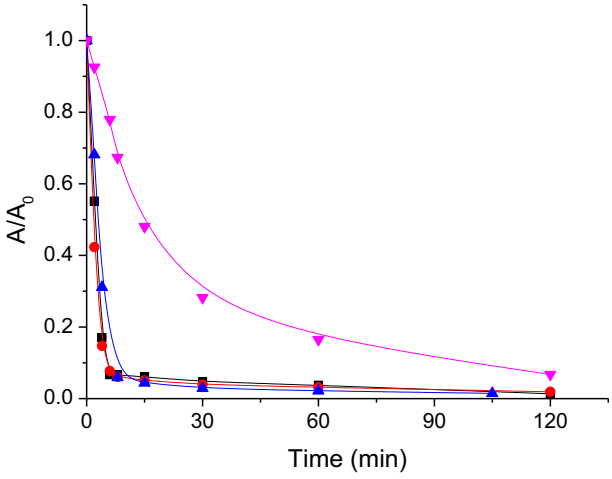

Fig. 12. Photodegradation of PRO dissolved in different water matrices in the presence of N.I.O. (1 g·L^{-1}) and OAA (2.0 mM) under UVA–Vis irradiation. Distilled water (■, pH = 3.0), river water (●, pH = 2.7), sewage (▲, pH = 3.4), and seawater (▼, pH = 3.5). T = 298 K.

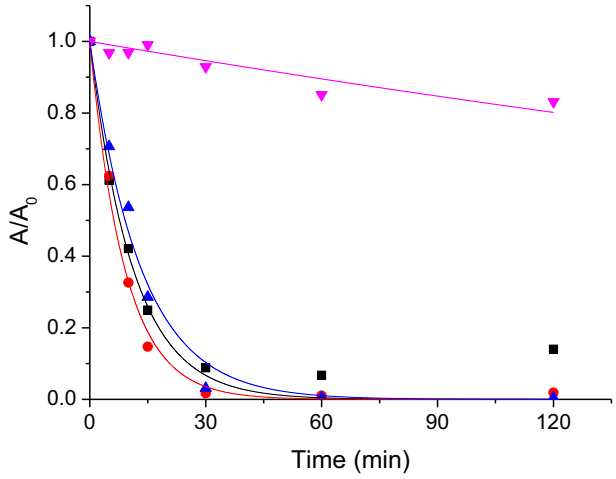

Fig. 13. Photodegradation of PRO dissolved in different water matrices in the presence of N.I.O. (1 g·L^{-1}) and OAA (2.0 mM) under sunlight. Distilled water (■, pH = 3.0), river water (●, pH = 2.7), sewage (▲, pH = 3.4), and seawater (▼, pH = 3.5). T *ca.* 298 K. All data were fitted to first-order kinetics equation.

Table 4
First-order kinetic rate constants (k·10^6 s^{-1}) obtained for the photodegradation of 8 ppm PRO in the presence of N.I.O. (1 g·L^{-1}) and OAA (2.0 mM) at natural pH. Experiments performed with either UVA–Vis lamp or sunlight, and different aqueous matrices.

Radiation		Matrix			
		Distilled water	River water	Sewage	Seawater
Lamp		6158 ± 515	7325 ± 419	4384 ± 378	717 ± 54
Sunlight	December	1501 ± 159	1853 ± 92	1263 ± 90	31 ± 4
	October (1)	1163 ± 148	1449 ± 183	1014 ± 108	26 ± 3
	October (2)	2028 ± 161	1780 ± 126	1032 ± 62	17 ± 1

3.9. *Reusability of N.I.O. usnder real conditions*

The system studied in this work has also been verified under other slightly different real conditions. Again, the elimination of the model pollutant PRO in distilled water, river water, sewage, and seawater was tested with sunlight at a different period of the year, October -Table 4 October (1)-, employing the same initial concentration of chemicals as above (Fig. 13). Furthermore, N.I.O. was recovered after this first use and it was reused again the day after -Table 4 October (2)- under the same conditions, but the solar radiation, which was quite different. Results obtained are shown in Fig. 14, while the radiation profiles during the solar experiments are collected in Fig. 15.

Results obtained in the first use of N.I.O. in October were slower than in December (Table 4). The elimination of PRO is very fast. Thus, 39% of PRO was degraded in just the first 5 min in distilled water (December), and this value increased to 58% after 10 min. However, the same

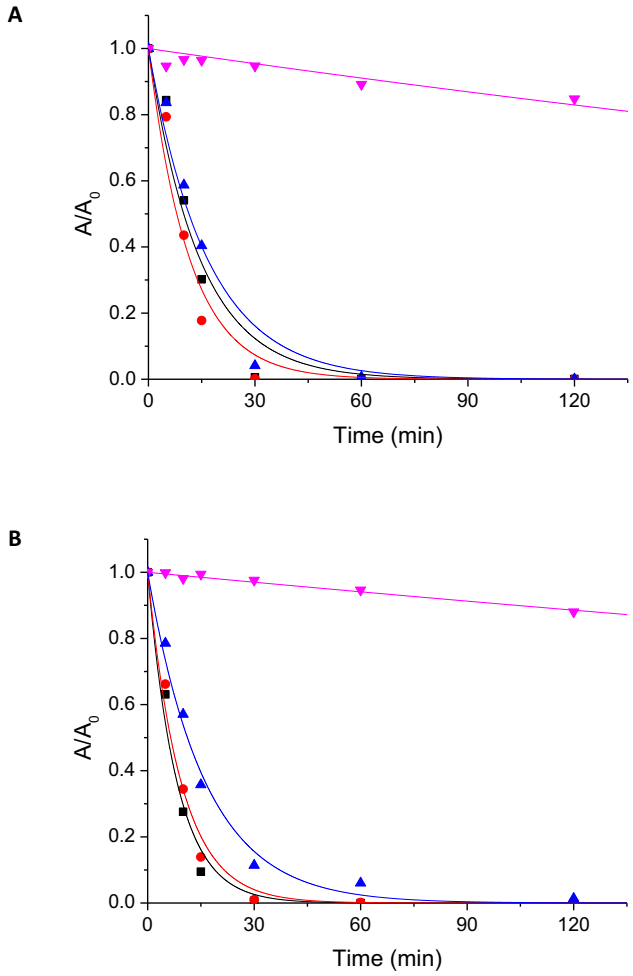

Fig. 14. Photodegradation of PRO dissolved in different water matrices in the presence of N.I.O. (1 g·L^{-1}) and OAA (2.0 mM) under sunlight; first (A) and second (B) use of N.I.O. Distilled water (■, pH = 2.8), river water (●, pH = 2.8), sewage (▲, pH = 3.0), and seawater (▼, pH = 3.4). T *ca.* 298 K. All data were fitted to first-order kinetics equation.

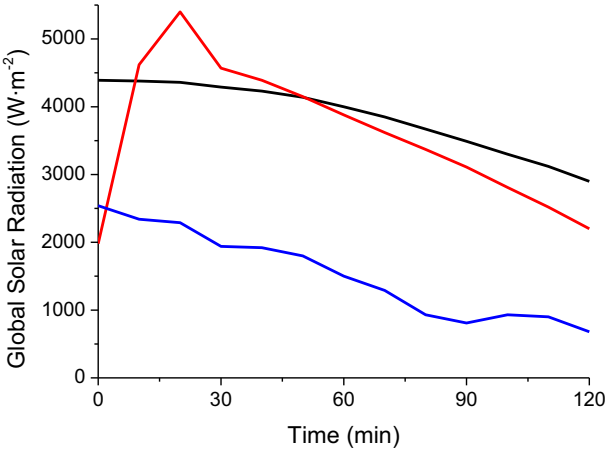

Fig. 15. Global solar incident radiation measured during the experiments with sunlight. December (—), and October 1st (—) and 2nd runs (—). These data were obtained from a neighboring meteorological station.

degradation only amounted to 16 and 46%, respectively, in October, due to the lower incident radiation on the photoreactor in the initial part of the reaction (Fig. 15). This applies to the four matrices employed, but the rates are sorted likewise: river water > distilled water > sewage ≫ > seawater. Conversely, the second run with the same photocatalyst was much faster than the other two experiments, despite the incident radiation was considerably lower (this day it was cloudy).

It has been observed that the settling rate of N.I.O. notably depends on the nature of the aqueous matrix. This different behavior was detected when the catalyst was recovered but it also happened during kinetic runs. Thus, the clay kept easily suspended in distilled water for a long time, and similarly in seawater. However, it settled quickly in river water and, particularly, in sewage. The latter has been collected from the inlet of a treatment plant that receives inflows of both domestic sewage and industrial wastewater, so it is a complex mixture of organic matter with other organic and inorganic chemicals. Therefore, any substance present in this matrix could have a flocculation effect or could promote the aggregation of particulate in any other way. On the other hand, river water should not promote the settling of N.I.O. The effect of organic species with high molecular weight, such as humic acids, on the settling rate of red mud, an industrial waste with high iron oxide content, has already been examined. [81] According to this study, N.I.O., a clay mostly composed of hematite, should present slower settling rate in river water than in distilled water, the opposite of what happened here.

This dissimilar settling behavior has two important effects. The first of them is that N.I.O. suspensions in river water and sewage already in the first use are less turbid. Thus, sunlight may reach the whole reaction vessel, enhancing photo Fenton reaction with dissolved iron cations. Apart from the previous discussion above (Section 3.8), this could also support the high elimination rates obtained in these two aqueous matrices (Table 4), despite they contain much greater amounts of degradable organic matter. The second outcome is related to the recovery of the catalyst. Following the procedure described in Section 2.4, the smaller particulate still in suspension after 2 h is discarded with the supernatant. Thus, a higher amount of fine N.I.O. was removed in the matrices where settling was slower, *i.e.* the effect is maximum with distilled water and minimum with sewage. Recovered catalyst samples led to suspensions with lower turbidity, as the smaller particles have been removed and the remaining N.I.O. settled easily, even under vigorous stirring. Therefore, the second use of N.I.O. in all matrices (but seawater, where only slight degradation occurs) revealed much faster than the first one (Table 4), despite the radiation received in the second run was considerably lower (Fig. 15). Furthermore, degradation rate particularly increased in distilled water, where settling was the slowest, and only very slightly in sewage, which showed much faster settling.

It must be taken into account that N.I.O. is a very affordable material. From an economic point of view its reuse is only acceptable if the recovery process is easy and costless. N.I.O. is a natural clay with high density and, therefore, it settles easily. A minor presence of iron oxide particles in water does not possess toxicity risk to the environment or any adverse outcome to human health, provided that they are not nanoparticles, [82] which is the case here, the granulometric analysis did not observe particles under 100 nm in the sample.

4. Conclusions

Propanolol (PRO) photodegradation is speeded up in acid media in the presence of suspended natural iron oxide (N.I.O.) and dissolved oxalic acid (OAA). PRO decomposes following first-order kinetics, faster with higher OAA concentration, and lower pH value and load of N.I.O. The addition of *t*-BuOH inhibits the photodegradation, *i.e.* this process takes place mostly *via* generated HO$^{\bullet}$. Besides the fast removal of the target compound, a relevant advantage with respect to standard photo-Fenton process was the observed neutralization of the initial acid pH along the reaction. Although PRO disappears in nearly 10 min under optimal conditions, TOC decreases much more slowly and *ca.* 40% TOC

remains after 3 h irradiation. Ten intermediates were identified in PRO photodegradation using HPLC/MS, and the corresponding reaction mechanism is proposed.

PRO photodegradation, employing this photo-Fenton-like system (N.I.O. & OAA with UVA–is radiation), accelerated in river water relative to distilled water, but it was slower in sewage and seawater, almost one order of magnitude with the latter. Photodegradation revealed also quite effective when sunlight is used, except for seawater, despite this process was studied under very weak winter solar radiation. Therefore, this technology reveals as a very promising sustainable method for the abatement of organic pollutants in fresh water and sewage, using sunlight as irradiation source and N.I.O. and OAA as abundant and cheap reagents, with the first of them being also reusable.

CRediT authorship contribution statement

W. Remache: Investigation, Formal analysis, Writing – original draft, Writing – review & editing, Visualization. **D.R. Ramos:** Investigation, Formal analysis, Writing – original draft, Writing – review & editing, Visualization. **L. Mammeri:** Investigation, Writing – original draft. **H. Boucheloukh:** Investigation, Writing – original draft. **Z. Marín:** Investigation, Writing – original draft. **S. Belaidi:** Formal analysis, Writing – original draft. **T. Sehili:** Writing – review & editing, Funding acquisition. **J.A. Santaballa:** Formal analysis, Resources, Writing – original draft, Writing – review & editing, Visualization, Funding acquisition. **M. Canle:** Formal analysis, Resources, Writing – original draft, Writing – review & editing, Visualization, Funding acquisition.

Declaration of competing interest

The authors declare that they have no known competing financial interests or personal relationships that could have appeared to influence the work reported in this paper.

Acknowledgments

The authors acknowledge the financial support of the Ministry of Higher Education and Scientific Research of Algeria (Project B00L01UN250120210003) and for research visits of WR and HB to UDC. This research was partially supported by the React! Group at UDC, and funded by the Spanish *Ministerio de Economía y Competitividad* through project CTQ2015-71238-R (MINECO/FEDER), and the *Xunta de Galicia* (Project GPC ED431B 2020/52), respectively. Funding for open access publication was provided by Universidade da Coruña/CISUG.

References

[1] T.E. Doll, F.H. Frimmel, Fate of pharmaceuticals—photodegradation by simulated solar UV-light, Chemosphere. 52 (2003) 1757–1769, https://doi.org/10.1016/S0045-6535(03)00446-6.

[2] M.L. Canle, M.I. Fernandez, C. Martinez, J.A. Santaballa, (Re)Greening photochemistry: using light for degrading persistent organic pollutants, Rev. Environ. Sci. Bio-Technology. 11 (2012) 213–221, https://doi.org/10.1007/s11157-012-9275-x.

[3] J.G. Hardman, L.S. Goodman, A. Gilman, Goodman & Gilman's, The Pharmacological Basis of Therapeutics, 9th ed., McGraw-Hill, New York, 1996, ISBN 978-0070262669.

[4] S.P. Kane, ClinCalc.com. https://clincalc.com/DrugStats/Drugs/Propranolol, 2021. (Accessed 12 November 2021).

[5] V. Gabet-Giraud, C. Miège, J.M. Choubert, S.M. Ruel, M. Coquery, Occurrence and removal of estrogens and beta blockers by various processes in wastewater treatment plants, Sci. Total Environ. 408 (2010) 4257–4269, https://doi.org/10.1016/j.scitotenv.2010.05.023.

[6] A. Pal, K.Y.-H. Gin, A.Y.-C. Lin, M. Reinhard, Impacts of emerging organic contaminants on freshwater resources: review of recent occurrences, sources, fate and effects, Sci. Total Environ. 408 (2010) 6062–6069, https://doi.org/10.1016/j.scitotenv.2010.09.026.

[7] J.P. Sumpter, T.J. Runnalls, R.L. Donnachie, S.F. Owen, A comprehensive aquatic risk assessment of the beta-blocker propranolol, based on the results of over 600 research papers, Sci. Total Environ. 793 (2021), 148617, https://doi.org/10.1016/j.scitotenv.2021.148617.

[8] S. Aydin, M.E. Aydin, A. Tekinay, H. Kilic, Occurrence and environmental risk assessment of β-blockers in urban wastewater, Fresenius Environ. Bull. 26 (2017) 1800–1805.

[9] S. Franzellitti, S. Buratti, P. Valbonesi, A. Capuzzo, E. Fabbri, The β-blocker propranolol affects cAMP-dependent signaling and induces the stress response in Mediterranean mussels, *Mytilus galloprovincialis*, Aquat. Toxicol. 101 (2011) 299–308, https://doi.org/10.1016/j.aquatox.2010.11.001.

[10] L.H.M.L.M. Santos, A.N. Araújo, A. Fachini, A. Pena, C. Delerue-Matos, M.C.B.S. M. Montenegro, Ecotoxicological aspects related to the presence of pharmaceuticals in the aquatic environment, J. Hazard. Mater. 175 (2010) 45–95, https://doi.org/10.1016/j.jhazmat.2009.10.100.

[11] D.B. Huggett, B.W. Brooks, B. Peterson, C.M. Foran, D. Schlenk, Toxicity of select beta adrenergic receptor-blocking pharmaceuticals (B-blockers) on aquatic organisms, Arch. Environ. Contam. Toxicol. 43 (2002) 229–235, https://doi.org/10.1007/s00244-002-1182-7.

[12] E. Isarain-Chávez, R.M. Rodríguez, J.A. Garrido, C. Arias, F. Centellas, P.L. Cabot, E. Brillas, Degradation of the beta-blocker propranolol by electrochemical advanced oxidation processes based on Fenton's reaction chemistry using a boron-doped diamond anode, Electrochim. Acta 56 (2010) 215–221, https://doi.org/10.1016/j.electacta.2010.08.097.

[13] N. De la Cruz, R.F. Dantas, J. Giménez, S. Esplugas, Photolysis and TiO_2 photocatalysis of the pharmaceutical propranolol: solar and artificial light, Appl. Catal. B Environ. 130–131 (2013) 249–256, https://doi.org/10.1016/j.apcatb.2012.10.003.

[14] M. Canle López, M.I. Fernández, C. Martínez, J.A. Santaballa, Photochemistry for pollution abatement, Pure Appl. Chem. 85 (2013) 1437–1449, https://doi.org/10.1351/PAC-CON-13-01-10.

[15] R.M. Cornell, U. Schwertmann, The iron Oxides: Structure, Properties, Reactions, Occurences and Uses, Wiley-VCH, 2006, ISBN 978-3-527-60644-3.

[16] J.K. Leland, A.J. Bard, Photochemistry of colloidal semiconducting iron oxide polymorphs, J. Phys. Chem. 91 (1987) 5076–5083, https://doi.org/10.1021/j100303a039.

[17] L. Mammeri, T. Sehili, S. Belaidi, K. Djebbar, Heterogeneous photodegradation of 1-naphthol with natural iron oxide in water: influence of oxalic acid, Desalin. Water Treat. 54 (2015) 2324–2333, https://doi.org/10.1080/19443994.2014.899928.

[18] J. Bandara, J.A. Mielczarski, A. Lopez, J. Kiwi, 2. Sensitized degradation of chlorophenols on iron oxides induced by visible light: comparison with titanium oxide, Appl. Catal. B. 34 (2001) 321–333, https://doi.org/10.1016/S0926-3373(01)00225-9.

[19] B.C. Faust, M.R. Hoffmann, D.W. Bahnemann, Photocatalytic oxidation of sulfur dioxide in aqueous suspensions of α-Fe_2O_3, J. Phys. Chem. 93 (1989) 6371–6381, https://doi.org/10.1021/j100354a021.

[20] S. Belaidi, T. Sehili, L. Mammeri, K. Djebbar, Photodegradation kinetics of 2,6-dimetylphenol by natural iron oxide and oxalate in aqueous solution, J. Photochem. Photobiol. A Chem. 237 (2012) 31–37, https://doi.org/10.1016/j.jphotochem.2012.03.023.

[21] W. Remache, S. Belaidi, L. Mammeri, H. Mechakra, T. Sehili, K. Djebbar, Photocatalytic degradation of 2,4-dichlorophenol using natural iron oxide and carboxylic acids under UV and sunlight irradiation: intermediates and degradation pathways, Desalin. Water Treat. 70 (2017) 311–321, https://doi.org/10.5004/dwt.2017.20524.

[22] Z. Redouane-Salah, M.A. Malouki, B. Khennaoui, J.A. Santaballa, M. Canle, Simulated sunlight photodegradation of 2-mercaptobenzothiazole by heterogeneous photo-Fenton using a natural clay powder, J. Environ. Chem. Eng. 6 (2018), https://doi.org/10.1016/j.jece.2018.02.011.

[23] B. Khennaoui, F. Zehani, M.A. Malouki, R. Menacer, M.C. López, Chemical and physical characterization of a natural clay and its use as photocatalyst for the degradation of the methabenzthiazuron herbicide in water, Opt. 219 (2020), 165024, https://doi.org/10.1016/j.ijleo.2020.165024.

[24] B. Khennaoui, M.A. Malouki, M.C. López, F. Zehani, N. Boutaoui, Z.R. Salah, A. Zertal, Heterogeneous photo-Fenton process for degradation of azo dye: methyl orange using a local cheap material as a photocatalyst under solar light irradiation, Opt. 137 (2017) 6–16, https://doi.org/10.1016/j.ijleo.2017.02.081.

[25] H. Boucheloukh, W. Remache, F. Parrino, T. Sehili, H. Mechakra, The effect of natural iron oxide and oxalic acid on the photocatalytic degradation of isoproturon: a kinetics and analytical study, Photochem. Photobiol. Sci. 16 (2017) 759–765, https://doi.org/10.1039/c6pp00441e.

[26] F. Li, J. Chen, C. Liu, J. Dong, T. Liu, Effect of iron oxides and carboxylic acids on photochemical degradation of bisphenol a, Biol. Fertil. Soils 42 (2006) 409–417, https://doi.org/10.1007/s00374-006-0084-7.

[27] U. Lueder, B.B. Jørgensen, A. Kappler, C. Schmidt, Photochemistry of iron in aquatic environments, Environ Sci Process Impacts 22 (2020) 12–24, https://doi.org/10.1039/c9em00415g.

[28] B.A. Dekkiche, N. Debbache, I. Ghoul, N. Seraghni, T. Sehili, Z. Marín, J. A. Santaballa, M. Canle, Evidence of non-photo-Fenton degradation of ibuprofen upon UVA irradiation in the presence of Fe(III)/malonate, J. Photochem. Photobiol. A Chem. 382 (2019), https://doi.org/10.1016/j.jphotochem.2019.111976.

[29] I. Ghoul, N. Debbache, B.A. Dekkiche, N. Seraghni, T. Sehili, Z. Marín, J. A. Santaballa, M. Canle, Fe(III)-citrate enhanced sunlight-driven photocatalysis of aqueous carbamazepine, J. Photochem. Photobiol. A Chem. 378 (2019) 147–155, https://doi.org/10.1016/j.jphotochem.2019.04.018.

[30] T. Kayashima, T. Katayama, Oxalic acid is available as a natural antioxidant in some systems, Biochim. Biophys. Acta Gen. Subj. 1573 (2002) 1–3, https://doi.org/10.1016/S0304-4165(02)00338-0.

[31] S.O. Lee, T. Tran, Y.Y. Park, S.J. Kim, M.J. Kim, Study on the kinetics of iron oxide leaching by oxalic acid, Int. J. Miner. Process. 80 (2006) 144–152, https://doi.org/10.1016/j.minpro.2006.03.012.

[32] D.M. Mangiante, R.D. Schaller, P. Zarzycki, J.F. Banfield, B. Gilbert, Mechanism of ferric oxalate photolysis, ACS Earth Sp. Chem. 1 (2017) 270–276, https://doi.org/10.1021/acsearthspacechem.7b00026.

[33] P. Mazellier, B. Sulzberger, Diuron degradation in irradiated, heterogeneous iron/oxalate systems: the rate-determining step, Environ. Sci. Technol. 35 (2001) 3314–3320, https://doi.org/10.1021/es001324q.

[34] X. Wang, C. Liu, X. Li, F. Li, S. Zhou, Photodegradation of 2-mercaptobenzothiazole in the γ-Fe2O3/oxalate suspension under UVA light irradiation, J. Hazard. Mater. 153 (2008) 426–433, https://doi.org/10.1016/j.jhazmat.2007.08.072.

[35] C. Liu, F. Li, X. Li, G. Zhang, Y. Kuang, The effect of iron oxides and oxalate on the photodegradation of 2-mercaptobenzothiazole, J. Mol. Catal. A Chem. 252 (2006) 40–48, https://doi.org/10.1016/j.molcata.2006.02.036.

[36] G.V. Buxton, C.L. Greenstock, W.P. Helman, A.B. Ross, Critical review of rate constants for reactions of hydrated electrons, hydrogen atoms and hydroxyl radicals (˙OH/O⁻ in aqueous solution), J. Phys. Chem. Ref. Data 17 (1988) 513–886, https://doi.org/10.1063/1.555805.

[37] A. Eslami, M.R. Khavari Kashani, A. Khodadadi, G. Varank, A. Kadier, P.-C. Ma, S. Madihi-Bidgoli, F. Ghanbari, Sono-peroxi-coagulation (SPC) as an effective treatment for pulp and paper wastewater: focus on pH effect, biodegradability, and toxicity, J. Water Process Eng. 44 (2021) 102330, https://doi.org/10.1016/j.jwpe.2021.102330.

[38] R.F. Dantas, O. Rossiter, A.K.R. Teixeira, A.S.M. Simões, V.L. da Silva, Direct UV photolysis of propranolol and metronidazole in aqueous solution, Chem. Eng. J. 158 (2010) 143–147, https://doi.org/10.1016/j.cej.2009.12.017.

[39] Y. Chen, Z. Liu, Z. Wang, M. Xue, X. Zhu, T. Tao, Photodegradation of propranolol by Fe(III)–citrate complexes: Kinetics,mechanism and effect of environmental media, J. Hazard. Mater. 194 (2011) 202–208, https://doi.org/10.1016/j.jhazmat.2011.07.081.

[40] M.P. Makunina, I.P. Pozdnyakov, Y. Chen, V.P. Grivin, N.M. Bazhin, V.F. Plyusnin, Mechanistic study of fulvic acid assisted propranolol photodegradation in aqueous solution, Chemosph. 119 (2015) 1406–1410, https://doi.org/10.1016/j.chemosphere.2014.10.008.

[41] S. Belaidi, L. Mammeri, H. Mechakra, W. Remache, K. Benhamouda, S. Larouk, M. A. Kribeche, T. Sehili, UV and solar light induced natural iron oxide activation: characterization and photocatalytic degradation of organic compounds, Int. J. Chem. React. Eng. 17 (2019), https://doi.org/10.1515/ijcre-2018-0027.

[42] M.E.A. Kribéche, H. Mechakra, T. Sehili, S. Brosillon, Oxidative photodegradation of herbicide fenuron in aqueous solution by natural iron oxide α-Fe2O3, influence of polycarboxylic acids, Environ. Technol. 37 (2016) 172–182, https://doi.org/10.1080/09593330.2015.1065008.

[43] J.D. García-Espinoza, P. Mijaylova Nacheva, Effect of electrolytes on the simultaneous electrochemical oxidation of sulfamethoxazole, propranolol and carbamazepine: behaviors, by-products and acute toxicity, Environ. Sci. Pollut. Res. 26 (2019) 6855–6867, https://doi.org/10.1007/s11356-018-4020-9.

[44] Y. Zuo, Kinetics of photochemical/chemical cycling of iron coupled with organic substances in cloud and fog droplets, Geochim. Cosmochim. Acta 59 (1995) 3123–3130, https://doi.org/10.1016/0016-7037(95)00201-A.

[45] G. Eisenberg, Colorimetric determination of hydrogen peroxide, Ind. Eng. Chem. Anal. Ed. 15 (1943) 327–328, https://doi.org/10.1021/i560117a011.

[46] M.A. Calatayud-Pascual, M. Sebastian-Morelló, C. Balaguer-Fernández, M. B. Delgado-Charro, A. López-Castellano, V. Merino, Influence of chemical enhancers and iontophoresis on the in vitro transdermal permeation of propranolol: evaluation by Dermatopharmacokinetics, Pharmaceutics 10 (2018) 265, https://doi.org/10.3390/pharmaceutics10040265.

[47] Q. Lan, H. Liu, F. Li, F. Zeng, C. Liu, Effect of pH on pentachlorophenol degradation in irradiated iron/oxalate systems, Chem. Eng. J. 168 (2011) 1209–1216, https://doi.org/10.1016/j.cej.2011.02.017.

[48] Q. Lan, M. Cao, Z. Ye, J. Zhu, M. Chen, X. Chen, C. Liu, Effect of oxalate and pH on photodegradation of pentachlorophenol in heterogeneous irradiated maghemite system, J. Photochem. Photobiol. A Chem. 328 (2016) 198–206, https://doi.org/10.1016/j.jphotochem.2016.06.001.

[49] B. Sulzberger, H. Laubscher, Reactivity of various types of iron(III) (hydr)oxides towards light-induced dissolution, Mar. Chem. 50 (1995) 103–115, https://doi.org/10.1016/0304-4203(95)00030-U.

[50] P. Borer, B. Sulzberger, S.J. Hug, S.M. Kraemer, R. Kretzschmar, Photoreductive dissolution of Iron(III) (Hydr)oxides in the absence and presence of organic ligands: experimental studies and kinetic modeling, Environ. Sci. Technol. 43 (2009) 1864–1870, https://doi.org/10.1021/es801352k.

[51] J. Jeong, J. Yoon, pH effect on OH radical production in photo/ferrioxalate system, Water Res. 39 (2005) 2893–2900, https://doi.org/10.1016/j.watres.2005.05.014.

[52] F.B. Li, X.Z. Li, X.M. Li, T.X. Liu, J. Dong, Heterogeneous photodegradation of bisphenol a with iron oxides and oxalate in aqueous solution, J. Colloid Interface Sci. 311 (2007) 481–490, https://doi.org/10.1016/j.jcis.2007.03.067.

[53] B.H.J. Bielski, D.E. Cabelli, R.L. Arudi, A.B. Ross, Reactivity of HO2/O− 2 radicals in aqueous solution, J. Phys. Chem. Ref. Data 14 (1985) 1041–1100, https://doi.org/10.1063/1.555739.

[54] Schindler Cornell, Photochemical dissolution of goethite in acid/oxalate solution, Clay Clay Miner. 35 (1987) 347–352, https://doi.org/10.1346/CCMN.1987.0350504.

[55] W. Remache, L. Mammeri, T. Sehili, K. Djebbar, Effect of natural iron oxide, hydrogen peroxide, and oxalic acid on photochemical degradation of 2-chlorophenol, Sci. Technol. A 39 (2014) 119–124. http://revue.umc.edu.dz/index.php/a/article/view/607.

[56] M. Pera-Titus, V. García-Molina, M.A. Baños, J. Giménez, S. Esplugas, Degradation of chlorophenols by means of advanced oxidation processes: a general review, Appl. Catal. B Environ. 47 (2004) 219–256, https://doi.org/10.1016/j.apcatb.2003.09.010.

[57] S. Sortino, S. Petralia, F. Boscà, M. Miranda, Irreversible photo-oxidation of propranolol triggered by self-photogenerated singlet molecular oxygen, Photochem. Photobiol. Sci. 1 (2002) 136–140, https://doi.org/10.1039/B109232D.

[58] N. Peng, K. Wang, S. Lin, L. Wu, Effects of inorganic ions on the photolysis of propranolol in FA solution, Environ. Sci. Pollut. Res. Int. 25 (2018) 26069–26078, https://doi.org/10.1007/s11356-018-2585-y.

[59] Y. Chen, C. Hu, X. Hu, J. Qu, Indirect photodegradation of amine drugs in aqueous solution under simulated sunlight, Environ. Sci. Technol. 43 (2009) 2760–2765, https://doi.org/10.1021/es803325j.

[60] D.L. Sedlak, J. Hoigné, The role of copper and oxalate in the redox cycling of iron in atmospheric waters, Atmos. Environ. Part A, Gen. Top. 27 (1993) 2173–2185, https://doi.org/10.1016/0960-1686(93)90047-3.

[61] S. Wei, L. Liu, H. Li, J. Shi, Y. Liu, Z. Shao, Photodecolourization of orange II with iron corrosion products and oxalic acid in aqueous solution, Appl. Catal. A Gen. 417–418 (2012) 253–258, https://doi.org/10.1016/j.apcata.2011.12.045.

[62] C. Siffert, B. Sulzberger, Light-induced dissolution of hematite in the presence of oxalate. A case study, Langmuir 7 (1991) 1627–1634, https://doi.org/10.1021/la00056a014.

[63] D. Panias, M. Taxiarchou, I. Douni, I. Paspaliaris, A. Kontopoulos, Thermodynamic analysis of the reactions of iron oxides: dissolution in oxalic acid, Can. Metall. Q. 35 (1996) 363–373, https://doi.org/10.1016/S0008-4433(96)00018-3.

[64] J. Santiago-Morales, A. Agüera, M. del Gómez M., A.R. Fernández-Alba, J. Giménez, S. Esplugas, R. Rosal, Transformation products and reaction kinetics in simulated solar light photocatalytic degradation of propranolol using Ce-doped TiO_2, Appl. Catal. B Environ. 129 (2013) 13–29, https://doi.org/10.1016/j.apcatb.2012.09.023.

[65] Y. Gao, N. Gao, W. Wang, S. Kang, J. Xu, H. Xiang, D. Yin, Ultrasound-assisted heterogeneous activation of persulfate by nano zero-valent iron (nZVI) for the propranolol degradation in water, Ultrason. Sonochem. 49 (2018) 33–40, https://doi.org/10.1016/j.ultsonch.2018.07.001.

[66] Q.-T. Liu, H.E. Williams, Kinetics and degradation products for direct photolysis of β-blockers in water, Environ. Sci. Technol. 41 (2007) 803–810, https://doi.org/10.1021/es0616130.

[67] M.L. Wilde, W.M.M. Mahmoud, K. Kümmerer, A.F. Martins, Oxidation–coagulation of β-blockers by K2FeVIO4 in hospital wastewater: assessment of degradation products and biodegradability, Sci. Total Environ. 452–453 (2013) 137–147, https://doi.org/10.1016/j.scitotenv.2013.01.059.

[68] V. Romero, N. De la Cruz, R.F. Dantas, P. Marco, J. Giménez, S. Esplugas, Photocatalytic treatment of metoprolol and propranolol, Catal. Today 161 (2011) 115–120, https://doi.org/10.1016/j.cattod.2010.09.026.

[69] A. Piram, R. Faure, H. Chermette, C. Bordes, B. Herbreteau, A. Salvador, Photochemical behaviour of propranolol in environmental waters: the hydroxylated photoproducts, Int. J. Environ. Anal. Chem. 92 (2012) 96–109, https://doi.org/10.1080/03067319.2010.497920.

[70] P. Xie, L. Zhang, J. Chen, J. Ding, Y. Wan, S. Wang, Z. Wang, A. Zhou, J. Ma, Enhanced degradation of organic contaminants by zero-valent iron/sulfite process under simulated sunlight irradiation, Water Res. 149 (2019) 169–178, https://doi.org/10.1016/j.watres.2018.10.078.

[71] H. Yang, T. An, G. Li, W. Song, W.J. Cooper, H. Luo, X. Guo, Photocatalytic degradation kinetics and mechanism of environmental pharmaceuticals in aqueous suspension of TiO_2: a case of β-blockers, J. Hazard. Mater. 179 (2010) 834–839, https://doi.org/10.1016/j.jhazmat.2010.03.079.

[72] Q.T. Liu, T.D. Williams, R.I. Cumming, G. Holm, M.J. Hetheridge, R. Murray-Smith, Comparative aquatic toxicity of propranolol and its photodegraded mixtures: algae and rotifer screening, Environ. Toxicol. Chem. 28 (2009) 2622–2631, https://doi.org/10.1897/09-071.1.

[73] L.A. Ioannou, E. Hapeshi, M.I. Vasquez, D. Mantzavinos, D. Fatta-Kassinos, Solar/TiO_2 photocatalytic decomposition of β-blockers atenolol and propranolol in water and wastewater, Sol. Energy 85 (2011) 1915–1926, https://doi.org/10.1016/j.solener.2011.04.031.

[74] Y.Q. Gao, N.Y. Gao, D.Q. Yin, F.X. Tian, Q.F. Zheng, Oxidation of the β-blocker propranolol by UV/persulfate: effect, mechanism and toxicity investigation, Chemosphere 201 (2018) 50–58, https://doi.org/10.1016/j.chemosphere.2018.02.158.

[75] R.G. Zepp, P.F. Schlotzhauer, R.M. Sink, Photosensitized transformations involving electronic energy transfer in natural waters: role of humic substances, Environ. Sci. Technol. 19 (1985) 74–81, https://doi.org/10.1021/es00131a008.

[76] R. Andreozzi, M. Raffaele, P. Nicklas, Pharmaceuticals in STP effluents and their solar photodegradation in aquatic environment, Chemosphere 50 (2003) 1319–1330, https://doi.org/10.1016/S0045-6535(02)00769-5.

[77] J. Mack, J.R. Bolton, Photochemistry of nitrite and nitrate in aqueous solution: a review, J. Photochem. Photobiol. A Chem. 128 (1999) 1–13, https://doi.org/10.1016/s1010-6030(99)00155-0.

[78] C.H. Liao, S.F. Kang, F.A. Wu, Hydroxyl radical scavenging role of chloride and bicarbonate ions in the H_2O_2/UV process, Chemosphere 44 (2001) 1193–1200, https://doi.org/10.1016/S0045-6535(00)00278-2.

[79] M. Krivec, R. Dillert, D.W. Bahnemann, A. Mehle, J. Štrancar, G. Drazic, The nature of chlorine-inhibition of photocatalytic degradation of dichloroacetic acid in a TiO_2-based microreactor, Phys. Chem. Chem. Phys. 16 (2014) 14867–14873, https://doi.org/10.1039/c4cp01043d.

[80] J. De Laat, G.T. Le, B. Legube, A comparative study of the effects of chloride, sulfate and nitrate ions on the rates of decomposition of H_2O_2 and organic compounds by Fe(II)/H_2O_2 and Fe(III)/H_2O_2, Chemosphere 55 (2004) 715–723, https://doi.org/10.1016/j.chemosphere.2003.11.021.

[81] X. Yanly, B. Shiwen, Z. Yun, L. Zijian, The effect of organics on the settling of red mud slurry, light metals: proceedings of sessions, in: TMS Annual Meeting, Pennsylvania, Warrendale, 2001, pp. 79–82.

[82] T.G. Kornberg, T.A. Stueckle, J.A. Antonini, Y. Rojanasakul, V. Castranova, Y. Yang, L. Wang, Potential toxicity and underlying mechanisms associated with pulmonary exposure to iron oxide nanoparticles: conflicting literature and unclear risk, Nanomater. 7 (2017) 307, https://doi.org/10.3390/nano7100307.